A SIMPLE FINITE METHOD FOR STRESS CONCENTRATION PROBLEMS IN PRESSURE VESSELS

E. GIENCKE,

Lehrstuhl für Konstruktionslehre,
Technische Universität Berlin, Berlin, Germany

ABSTRACT

The application of a simple finite method for solving stress concentration problems in pressures vessels will be shown. In contrary to the finite element method stresses and not deformations or stress functions will be introduced as unknowns. Thus the loss of accuracy by deriving the stresses from the deformations and stress functions will be avoided. Equilibrium and compatibility can be satisfied by the principles of virtual work. By introducing special virtual displacements and forces only line integral must be solved. Therefore it is possible to utilize special approximations for the stresses near the stressconcentration points for reducing the number of unknowns without lost of accuracy. Some examples as perforated plates and shells, intersections of tubes with perforated plates shells will be discussed.

1. Introduction

Calculations of stress concentrations problems, as for example for cut-outs in pressure vessels by means of finite methods usually require a great effort. The stress peaks at the holes, can only be analized by a relatively fine grid,(it is shown in figure 1a). From experience it is known, that the finite method are less accurate if stress peaks occur on boundaries, since the accuracy of boundary equations is at least one order lower than that of the equations for the inner points. When using the deformation method a lot of accuracy gets lost at the calculation of stresses, since the strains must be calculated from the displacements by means of a numerical differentiation process. At the boundary non-symmetric differences must be used, which again are known to be one order lower in accuracy than the symmetrical differences for inner points. For a stretched plate with a hole, a grid as fine as shown at the left in figure 1a is necessary. In the following a simple method will be presented which is very transparent and very accurate also, so that the coarse rectangular grid at the right in figure 1a is sufficient. As unknowns the normalforces and bending moments are introduced directly so that the differentiationprocess just mentioned is not necessary |1,2|.

2. Finite Equations for plate-stretching

To get an impression, how this method works, first the equilibrium and compatibility equations for a regular inner point in a stretched plate will be derived. A complete representation of this method is given in |1,2|. Since we establish equations for an approximated stress distribution it is approbiate to use an energy statement, that means the principles of virtual displacements and forces. The establishment of the equations can be simplified by using virtual displacements and forces simple as possible.

For deriving the equilibrium equation for plate stretching, we introduce the simple virtual displacement according to figure 2a by rotating the four fields as rigid bodies about the corner points. The four elements overlap at the center line and break down from the neighbouring elements on the outer lines. The corresponding discontinuities δs_x, δs_y of the displacements are shown in figure 2a. Someone might object that the virtual displacements are not geometrically compatible, because there are gaps and overlappings in the displacements. But the principle of virtual displacements only demands, that the displacements are compatible within the elements. If there are discontinuities at their boundaries, then the interior forces act there as external loads. Due to the discontinuities δs_x and δs_y only the real normal forces at the grid lines produce a virtual work

$$\delta W_e = \int n_x \, \delta s_x \, dy + \int n_y \, \delta s_y \, dx. \qquad (1)$$

The shear forces do not produce virtual work, because the tangential deformations at the grid lines are the same. The external work (1) must vanish, because we have not virtual strains and therefore no internal work δW_i.

By introducing these virtual displacements we have, when calculating the virtual work (1) only integrations along the gridlines and not over the surface of the elements. This is of great advantage, because it is sufficient to express the distribution of the normal forces only along the gridlines and not over the whole element as in the conventional methods. If the equation will be restricted to an influence zone of 3 by 3, the best approximation for the distribution of the real normal forces is a parabola that means, a second order Lagrangian polynomial through three neighbouring nodal points, which can be written as a finite Taylor expansion

$$f(x) = \left\{ \begin{bmatrix} \cdot & \boxed{1} & \cdot \end{bmatrix} + \begin{bmatrix} -1 & \boxed{\cdot} & 1 \end{bmatrix} \frac{x}{2\,h} + \begin{bmatrix} 1 & \boxed{-2} & 1 \end{bmatrix} \frac{x^2}{h^2} \right\} f. \qquad (2)$$

For the integration of a product of the real normal force distribution of (2) with a triangular virtual displacement δs (with the peak value 1) we obtain the operator $\begin{bmatrix} 1 & \boxed{10} & 1 \end{bmatrix}$ $fh/12$. The difference $\begin{bmatrix} 1 & \boxed{-2} & 1 \end{bmatrix}$ in the other direction of the difference scheme (3) results automatically, because the displacements on the center line are twice as large and opposite to those on the outer lines.

The virtual work of the normalforces n_x is summarized in the first difference scheme (3) and that of the normalforces n_y in the second scheme

$$\begin{bmatrix} -1 & 2 & -1 \\ -10 & \boxed{20} & -10 \\ -1 & 2 & -1 \end{bmatrix} \begin{Bmatrix} N_x \\ \kappa_y \end{Bmatrix} \frac{k}{h} - \begin{bmatrix} -1 & -10 & -1 \\ 2 & \boxed{20} & 2 \\ -1 & -10 & -1 \end{bmatrix} \begin{Bmatrix} N_y \\ \kappa_x \end{Bmatrix} \frac{h}{k} = 0 \,. \qquad (3)$$

This equation is a difference equation of higher order for the equilibrium condition $n_x'' - n_y'' = 0$. In a complete dual way we find the compatibility equation for the bending curvatures κ_x and κ_y. The accuracy of the equation (3) is very well, because we are able to represent a parabolic stress distribution only with one unknown per nodalpoint.

In order to satisfy the compatibility for the strains we have to utilize the principle of virtual forces. The most simple virtual force system restricted to four elements is the wellknown equilibrium group of a shearpanel - structure (figure 2b). The work of the corresponding virtual normal forces δN_x, δN_y (*) at the real extensions ε_x and ε_y is

(*) In contrast to the distributed forces and stiffnesses of the plate, concentrated forces or forces and stiffnesses of beams and stringers will be indicated by capitals.

$$\int \varepsilon_x \, \delta N_x dx + \int \varepsilon_y \, \delta N_y \, dy = \begin{vmatrix} -1 & -10 & -1 \\ 2 & \boxed{20} & 2 \\ -1 & -10 & -1 \end{vmatrix} \frac{\varepsilon_x h}{12k} +$$

$$+ \begin{vmatrix} -1 & 1 & -1 \\ -10 & \boxed{20} & -10 \\ -1 & 2 & -1 \end{vmatrix} \frac{\varepsilon_y k}{12h} \, . \qquad (4)$$

Again the real extensions are approximated by a parabolic distribution (2) along the lines. Because the virtual normal forces are concentrated on the gridlines we only obtain here integrals along the gridlines.

The only surface integral $\iint \gamma_{xy} \delta n_{xy} \, dxdy$ is the work of the virtual shear force δn_{xy} (figure 2b) on the real shear γ_{xy}. Because the shear strains are not the unknowns, we have to eliminate them. In the principle of virtual work the shear strains $\gamma_{xy} = 2 f_s n_{xy}$ will be substituted by the shear forces n_{xy} by means of the stress-strain relationship. Furthermore a virtual shear strain $\delta\gamma_{xy}$ will be chosen equal to the virtual shear force δn_{xy} according to figure 2c. Thus we are able to express the shear work $\iint \gamma_{xy} \delta n_{xy} \, dxdy$ by a shear work in the principle of virtual displacements

$$\iint \gamma_{xy} \, \delta n_{xy} \, dxdy \equiv 2 \, f_s \iint n_{xy} \, \delta n_{xy} \, dxdy = 2 \, f_s \iint n_{xy} \delta\gamma_{xy} \, dxdy$$

and the last term by a corresponding normal force work. Or with other words we apply the principle of virtual forces and displacements both at once. If each principle is true

$$\delta W_i = \delta W_e \quad \text{and} \quad \delta W_i^* = \delta W_e^* \, ,$$

then the linear combination

$$\lambda \, \delta W_i + \lambda^* \delta W_i^* = \lambda \, \delta W_e + \lambda^* \delta W_e^* \qquad (5)$$

is also true. In our case we introduce the virtual forces according to figure 2b with the facotr $\lambda^* = 1$ and the virtual displacements according to figure 2c with the factor $\lambda = + f_s$. Then both shear works

$$\iint (\gamma_{xy} \, \delta n_{xy} + \underbrace{f_s \, n_{xy}}_{\gamma_{xy}/2} \, \delta\gamma_{xy}) \, dxdy$$

cancel each other because $\delta\gamma_{xy} = -2\,\delta n_{xy}$. The virtual work

$$\int \varepsilon_x \delta N_x dx + \int \varepsilon_y \delta N_y dy = + f_s\left(\int n_y \delta s_y dx + \int n_x \delta s_x dy\right)$$

or

$$\begin{vmatrix} -1 & -10 & -1 \\ 2 & \boxed{20} & -10 \\ -1 & -10 & -1 \end{vmatrix} \underbrace{(\varepsilon_x + f_s\, n_y)}_{f(n_x+n_y)} \frac{h}{12k} +$$

$$+ \begin{vmatrix} -1 & 2 & -1 \\ -10 & \boxed{20} & -10 \\ -1 & 2 & -1 \end{vmatrix} \underbrace{(\varepsilon_y + f_s\, n_x)}_{f(n_y+n_x)} \frac{k}{12h} = 0 \qquad (6)$$

remains. After consideration of the stress-strain relationships for the normalforces in an isotropic plate we get

$$\varepsilon_x + f_s\, n_y = \varepsilon_y + f_s\, n_x = f(n_x + n_y) = \frac{\varepsilon_x + \varepsilon_y}{1-\nu}$$

For the bending problem a similar equilibrium equation will be obtained. The extension sum $\varepsilon_x + \varepsilon_y$ then must be substituted by the moment sum $m_x + m_y$ and on the right hand side in (6) the virtual work $\int p\delta w\, dxdy$ of the vertical load p must be added. The advantage of this method is that because of the simple virtual states only lineintegrals must be evaluated. This fact we use with great success in the stress concentration problem. On the other hand because of the duality between plate stretching and bending the same set of equations can be used for the two problems.

3. Perforated plate

As first stress concentration problem, let us start with a perforated plate, which may be a tube sheet in a heat exchanger (figure 3). These tubesheets are strained by stretching and bending mainly, because they are clamped in the vessel walls. For the stress analysis of the pressure vessels the effective stretching- and bending stiffness of the perforated tube sheet and the stress concentration factors at the holes will be needed. Because of the regular perforation there are two axis of symmetry for the quadratic perforation as well as for the triangular perforation. Therefore the general problem can be reduced to a symmetric problem with tension in both directions and to a antisymmetric problem with tension in one direction and compression in the other (figure 1,5).

In order to concentrate us to the essential, the problem first will restricted to plane stretching considering first the influence of the tubes welded to the plate by a stiffness at the hole contour. Let us consider a plate with a quadratic perforation grid under uniform tension then the lines 1-2, 3-4, 2-3, 4-5, and the diagonals are axis of symmetry (figure 3). Because of the diagonal symmetry ($n_{x,1} = n_{y,5} \equiv n_1$, $n_{y,1} = n_{x,5} \equiv n_5$, $n_{x,2} = n_{y,4} \equiv n_2$, $n_{y,2} = n_{x,4} \equiv n_4$, $n_{x,3} = n_{y,3} \equiv n_3$) the only unknowns are the five normalforces n_x in the points 1 to 5 and the normalforce N_1 in the stiffness. We now still have to make assumptions on the normalforce distributions. On the line 1-2 a parabolic distributions will be assumed which is defined by the two values in the points 1 and 2 because of the symmetry in point 2

$$\text{line 1-2: } n_x(y) = n_2 + (n_1 - n_2) \left(\frac{y}{h'}\right)^2 . \qquad (7)$$

Because of the diagonal symmetry the normalforces n_y on the line 4-5 have the same distribution. On the line 3-4 the distribution will be superimposed by a constant function and a cosinefunction in order to take care of the symmetry-condition in the points 3 and 4. This distribution is also defined by the values in the points 3 and 4

$$\text{line 3-4: } n_x(y) = \frac{1}{2} \left|(n_3 + n_4) + (n_3 - n_4) \cos \frac{\pi y}{h}\right| . \qquad (8)$$

On the contour of the hole the strain $\varepsilon_s(s)$ in this coarse grid only can be constant, therefore also the normalforces n_s, n_r and the normalforce in the stiffner N are constant

$$n_s(s) = n_1, \; n_r(s) = n_5, \; N(s) = N_1 \quad .$$

For the six unknowns n_1 to n_5 and N_1 three equilibrium equations and three compatibility conditions must be formulated. At first we have to postulate that on the two lines 1-2 and 3-4 sum of the normalforces is equal to the resultant normalforce nh on one elementlength, or when using the principle of virtual displacements the constant virtual displacement $\delta u_1 = 1$ in the cross section 1-2 and $\delta u_2 = 1$ in the cross section 3-4 must be introduced (figure 4a). With the approximated normalforce distribution (7,8) we get the virtual work

$$\text{on line 1-2: } \delta W_e = N_1 + \int_1^2 n_x \, dy - nh = N_1 + (n_1 + 2n_2) \frac{h'}{3} - nh = 0 \qquad (9)$$

$$\text{on line 3-4: } \delta W_e = \int_3^4 n_x \, dy - nh = (n_3 + n_4) \frac{h}{2} - nh = 0. \qquad (10)$$

The third condition is the equilibrium between the normalforce $n_r = n_c$

at the boundary of the hole and the stiffnessnormalforce N_1

$$N_1 = n_r a = n_5 a \,. \tag{11}$$

In addition the extension of the stiffness $\varepsilon_s = N_1/EF$ and the extension of the boundary of the hole $\varepsilon_s = (n_s - \nu n_r)/Et$ is the same

$$\frac{N_1}{EF} = \frac{1}{Et}(n_1 - \nu n_5). \tag{12}$$

With equation (11) and the stiffnessquotient

$$\alpha = \frac{EF/Et\ a}{1+\nu EF/Et\ a} \tag{13}$$

the first compatibility equation follows finally from (12)

$$n_5 = \alpha\, n_1 = N_1/a \,. \tag{14}$$

Furthermore two compatibility conditions have to established. First, the two symmetrylines 1-2 and 3-4 must stay plain. In order to formulate this statement, we use the principle of virtual forces and introduce the virtual forces in figure 4b, which produce no external work. They generate virtual normalforces at the gridlines and virtual normalforces $\delta N_s = \sin\phi$ as well as virtual bending moments $\delta M_s = a \sin\phi$ at the contour of the hole. Because of these virtual bending moments the bending curvature κ_s of the hole contour has to be introduced as an additional unknown in general problems. An external work does not arise, since the sections 1-2 and 3-4 stay plain, so that the internal work

$$\delta W_i^* = \int \varepsilon_x\, \delta N_x\, dx + \int (\varepsilon_s\, \delta N_s + \kappa_s\, \delta M_s)\, ds = 0 \tag{15}$$

must vanish. When assuming a constant strain $\varepsilon_s(s)$ along the contour of the hole, as we have done in the case of our coarse grid, there is no elastic curvature κ_s possible. Thus the inner work is nothing else but the integral of the strains on the straight lines 1-2 and 3-4 and the boundary of the hole. If the extensions ε_x will be approximated in the same form (7,8) as the normalforces n_x, the integration (15) yields

$$\delta W_i^* = (2\varepsilon_4 + \varepsilon_5)\frac{h'}{3} - (\varepsilon_2 + \varepsilon_3)\frac{h}{2} + \varepsilon_1 a = 0. \tag{16}$$

Finally the compatibility of the displacements around the hole must be demanded. For this we introduce the virtual forces in figure 4c. To these virtual forces correspond linearly distributed normal forces along the grid lines and constant shears in the elements. In order to eleminate the shear

work, we simultaniously introduce virtual displacements which are chosen so, that the shearwork in both virtual works $\delta W_i^* + \lambda \delta W_i$ cancel each other as in equation (6) and the combined virtual work (5)

$$\int |\varepsilon_x \, \delta N_x + (1 + \nu)\delta s_y \, n_y/Et| \, ds \quad + \quad \int |\varepsilon_y \, \delta N_y + (1 + \nu)\delta s_x \, n_x/Et| \, dy$$

$$\int |\varepsilon_s \, \delta N_s + (1+\nu) \, \delta s_r \, n_r \, / \, Et| ds \quad = \quad 0$$

remains. Observing in figure 4c

$$\delta s_y = - \delta N_x, \; \delta s_x = - \delta N_y, \quad \delta s_r = - \delta N_s = \sin\phi - \frac{a}{h} \sin 2\phi$$

and the stress strain relationship for the strains as $\varepsilon_x = (n_x - \nu n_y)/Et$ the virtual work gets the clear form

$$\int (n_x + n_y) \, \delta N_x \, dx + \int (n_x + n_y) \, \delta N_y \, dy + \int (n_s + n_r) \, \delta N_s \, ds = 0 \qquad (17)$$

or after integration

$$\frac{1}{3} \left(1 - \frac{a}{h}\right)^2 (n_1 + n_5 + n_2 + n_4) - \frac{1}{2} \left(\frac{1}{2} + \frac{2}{\pi^2}\right) (n_2 + n_4) - \left(\frac{1}{2} - \frac{2}{\pi^2}\right) n_3$$
$$+ \frac{a}{2h}\left(1 - \frac{a}{2h}\right) (n_1 + n_5) \quad \text{with} \quad n_5 = \alpha n_1 . \qquad (17a)$$

Thus we have six equations (9,10,11,14,16,17) for the six unknowns.

It is favourable to work in the compatibility equations with the normalforcesum $n_x + n_y$ as unknown, since the normalforcesum and in the bending problem the momentsum $m_x + m_y$ has a smoother distribution than the normalforces themselve. That will be confirmed by the solution in a plate with one circular hole (figure 1b). In the symmetric case the peak of the normalforces growths due to a second order hyperbola and in the antisymmetric case even due to a fourth order hyperbola. The normalforces sum however is in the symmetric case constant and in the antisymmetric case increases only to a second order hyperbola.Such smoother distributions can be approximated piecewise parabolically quite well. Also in the compatibility equation (16) the extensionsum $\varepsilon_x + \varepsilon_y$ or the normalforcesum will be the unknown instead of ε_x, when introducing beside the virtual forces after figure 4c corresponding constant virtual displacements.

In the bending problem the procedure is analog. We get the same results as in the stretching problem, if the stiffness quotient α will be now defined as the quotient between the bending stiffness EI of the boundary stiffner and the plate stiffness b

$$\alpha = \frac{EI}{ba} \quad . \tag{18}$$

In figure 5 the results are represented, when the hole distance 2h is twice the hole diameter 2a. The stress peak at the hole boundary decreases with increasing stiffness of the boundary flange until the limit value of the so called "neutral" hole ($\alpha = 1$) with a constant state of stress. In the antisymmetric case (figure 5b) the stress peaks are more distinctive (see also figure 1b) so that it is more appropriate to substitute the parabolic term in the approximation (7) by a fourth order hyperbola

$$\text{line 1-2:} \qquad n_x(y) = a + b \left| \left(\frac{h}{h-y}\right)^4 + \left(\frac{h}{h+y}\right)^4 \right| , \tag{19}$$

which will be get for the stress distribution in a plate with one circular hole (figure 1). Equations (19) represents the superposition of the solutions for two holes with a distance 2h.

To include the variation of the stresses on the contour of the hole, we introduce point 6 (figure 3) as an additional point as well as the normalforce $n_{s,6} = n_6$ and the bending curvature $\kappa_{s,1} = \kappa_1$ as additional unknowns. The normalforce distribution on the line 3-6 will be approximated parabolically as in equation (7)

$$n(x') = n_3 + (n_6 - n_3) \left(\frac{x'}{\sqrt{2}h'}\right) \quad . \tag{20}$$

On the circular boundary the normalforces have a periodic form

$$n_s(\phi) = \frac{1}{2} \left| (n_1 + n_6) + (n_1 + n_6) \cos 4\phi \right| \tag{21}$$

with the corresponding bending curvature about the z-axis

$$\kappa_s(\phi) = \kappa_1 \cos 4\phi \quad . \tag{22}$$

For the new unknwons we have to formulate an euqilibrium equation by means of the virtual displacements in figure 4d with the virtual work

$$(n_3 - 2n_6) \frac{\sqrt{2}h'}{3} \frac{1}{\sqrt{2}} = nh \tag{23}$$

and a compatibility equation with the virtual forces in figure 4d.

The comparison with results by the method of conformial mapping |3| for a perforated plate without boundary stiffner is quite well. The values in |3| are $n_1 = 2{,}668\ n$ and $n_6 = 2{,}318\ n$, we get in the first case with a

constant stress on the hole contour $n_1 = n_6 = 2{,}50$ n and after introducing the unknowns n_6 and κ_1 the better values $n_1 = 2{,}67$ n and $n_6 = 2{,}33$ n. In the antisymmetric case the stress peak is $n_1 = 3{,}89$ n in comparison to 3,887 n in |3|.

When including the effect of the tubes the stretching and bending problem is coupled because the boundary forces between the plate and the tubes do not only effect a radial displacements but also a rotation of the tube-ends. In the symmetric case the number of unknowns in our coarse grid then are 12, 6 normalforces and 6 bending moments. If the tube sheet is curved, shell terms must included. For a shallow shell the equilibrium equations for the stretching forces and the compatibility equations for the elastic curvatures are the same as for a plane plate. Shell-terms must be added in the equilibrium equation for the moments and the compatibility equation for the stretching strains |4|. In figure 7 is shown how the shell terms will be introduced into the compatibility equation (16) of the stretching problem. To derive this equation we put the virtual forces in figure 4b to the plate.These virtual forces produce constant normalforces along the grid lines as we have seen before (figure 4b). When this gridline is on a shell, then the line is curved and deviationforces $p_z = 1/r$ (figure 7a) will be needed. These deviationforces are compensated by bending in x and y-direction, in order to satisfy the equilibrium (figure 7b). These virtual bending moments δM_x, δM_y, δM_s , which are proportional to the curvature $\frac{1}{r}$ of the shell, works at the elastic curvatures κ_x, κ_y at the gridlines and $\bar{\kappa}_s$ at the hole |5|

$$\delta W_i^* = \int \kappa_x \delta M_x dx + \int \kappa_y \delta M_y dy + \int \bar{\kappa}_s \delta \bar{M}_s ds. \qquad (24)$$

The curvature $\bar{\kappa}_s$ and the moment $\delta \bar{M}_s$ are rotating about an axis in the plane of the shell and not about the z-axis as in the stretching problem as before.

To get an impression how the tubes and the curvatures of the sheet influence the stress distribution, in figure 6 the stress distributions for a plane plate without tubes (....), for a plane plate with tubes (---) and for a spherical curved plate with tubes (——) are represented. Due to the tubes and the plate curvature the stress peak decreases, because the tubes stiffen the holes of the plate but in the shell this stiffening effect is larger, because the shell is weaker than the plate.

4. Conclusion

In the future perforated plate with a triangular arrangement of the holes will be to investigated as well as plates and shells with single nozzles and cutouts. In this case only regular equations must included into the analysis. Finally for thick plates, the plate theory is inadequate, and threedimensio-

nal theory must be used . The method shown here can be appropriately applied as well |6|.

The presented method differs from the usual methods of finite elements in three major points:

1. In the selection of the unknowns: They are not self equilibrated force groups or displacements, but they are rather the normaforce and the bending curvatures.
2. Virtual and real forces and displacements respectively do not coincide with each other as in the usual methods. The most simple virtual states are shosen, that virtual work only exists at the gridlines. Therefore we are able to handle easily different approximations like (7,8,19,21,22) at the several gridlines.
3. Both principles of virtual work are applied simultaneaously for the elimination of the shear forces and twisting curvatures by introducing virtual forces and displacements at the same time.

5. Literature

|1| Giencke, E. — Ein einfaches und genaues finites Verfahren zur Berechnung von orthotropen Scheiben und Platten, Stahlbau 36 (1967), S. 260-268 und 303-315.

Giencke, E. — The mechanical interpretation of high accuracy multipoint difference methods for plates and shells, IUTAM Symposium on "High speed computing of elastic structures, Liège, August 1970, Published as Volume 81 of Le congrès et colloques de L"universite de Liège, 1971.

|2| Giencke, E. — Lösung von Ausschnittproblemen mit einem speziellen finiten Verfahren. ZAMM 50 (1970), T 117-119.

Hieronimus, K. — Ein Beitrag zur Berechnung krummlinig berandeter Scheiben. Dissertation, TU Berlin, 1971.

|3| Meijers, P. — Doubly-periodic stress distributions in perforated plates. Dissertation T.U. Delft, 1967.

|4| Marguerre, K. — Neue Festigkeitsprobleme des Ingenieurs, Springer-Verlag, Berlin, 1950.

|5| Giencke, E. — Ein einfaches finites Verfahren zur Berechnung von Flächentragwerken, V. IKM 1969, Wissenschaftliche Zeitschrift der Hochschule für Architektur und Bauwesen, Weimar 16 (1969), S. 231-234.

|6| Giencke, E. — Ein einfaches finites Verfahren zur Berechnung räumlicher Elastizitätsprobleme. Zeitschrift für Flugwissenschaften (ZFW) 16 (1968), S. 179-183, 277-291

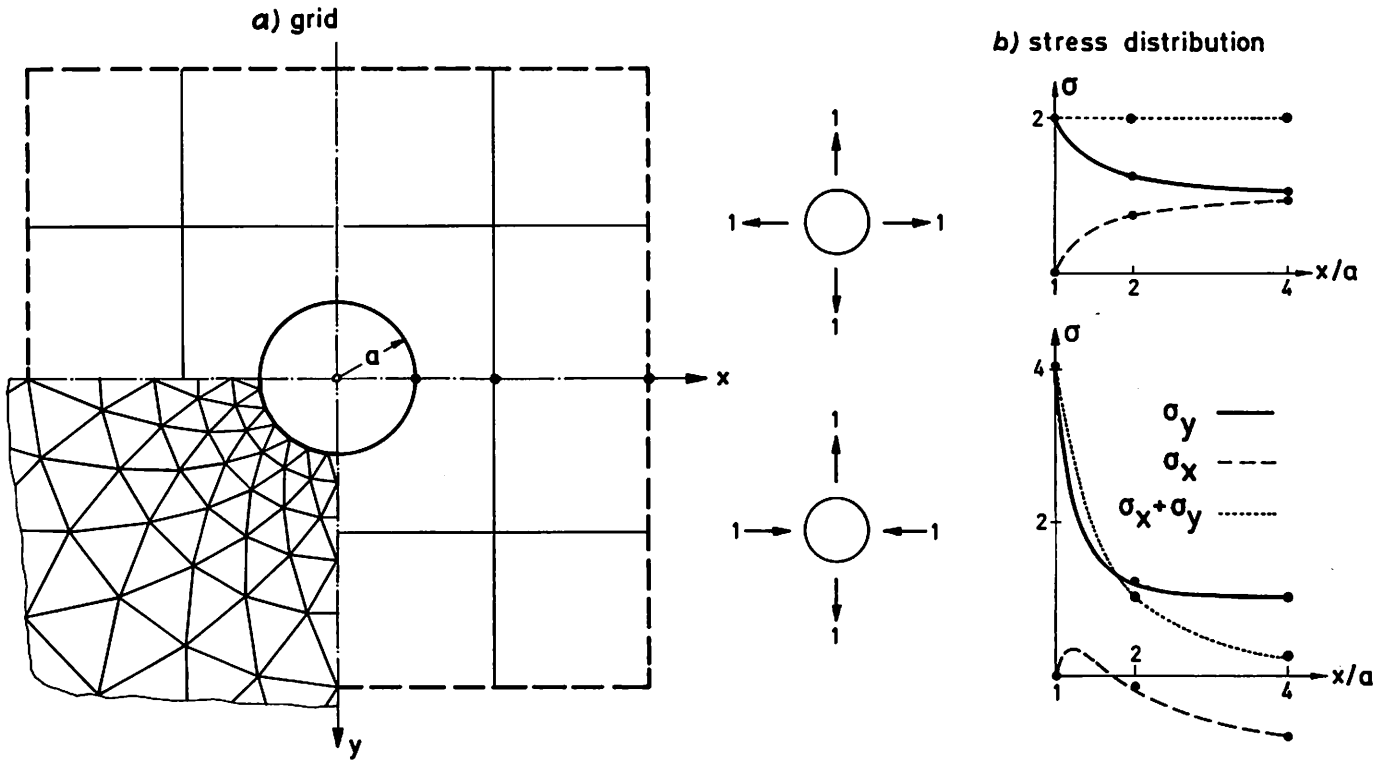

Figure 1: Plate with circular hole

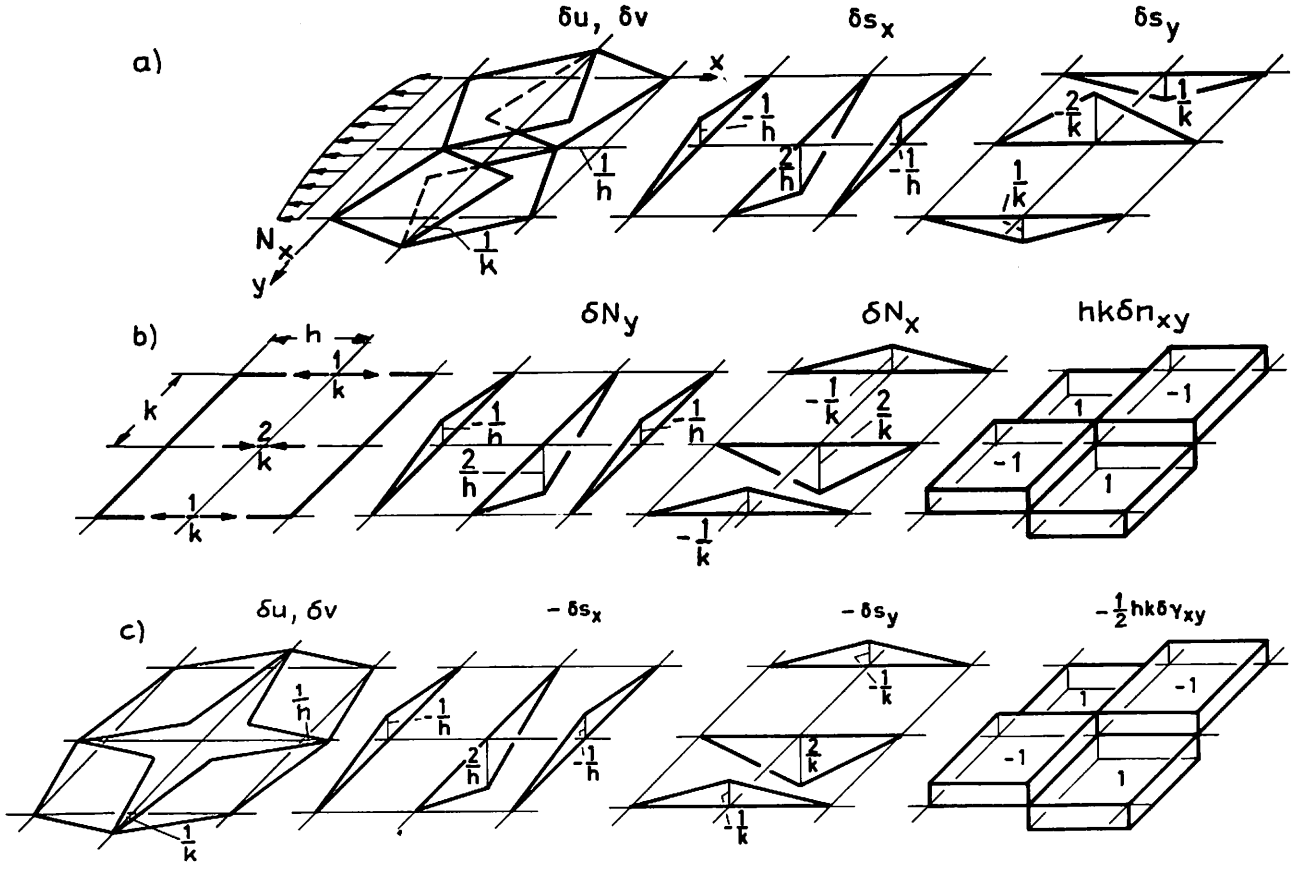

Figure 2: Virtual displacements and forces for plate stretching.

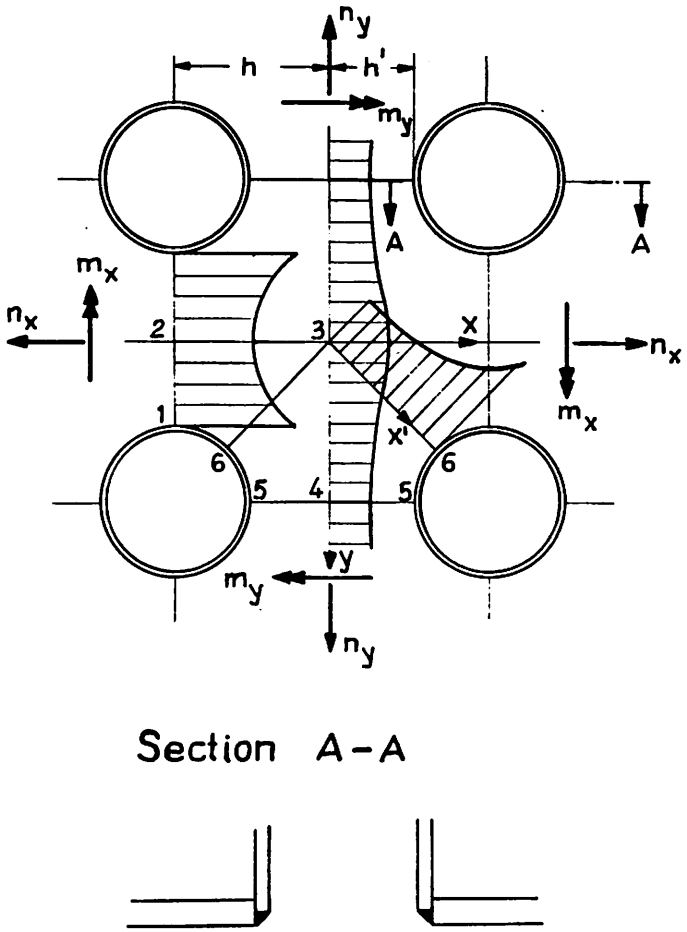

Figure 3. Perforated plate

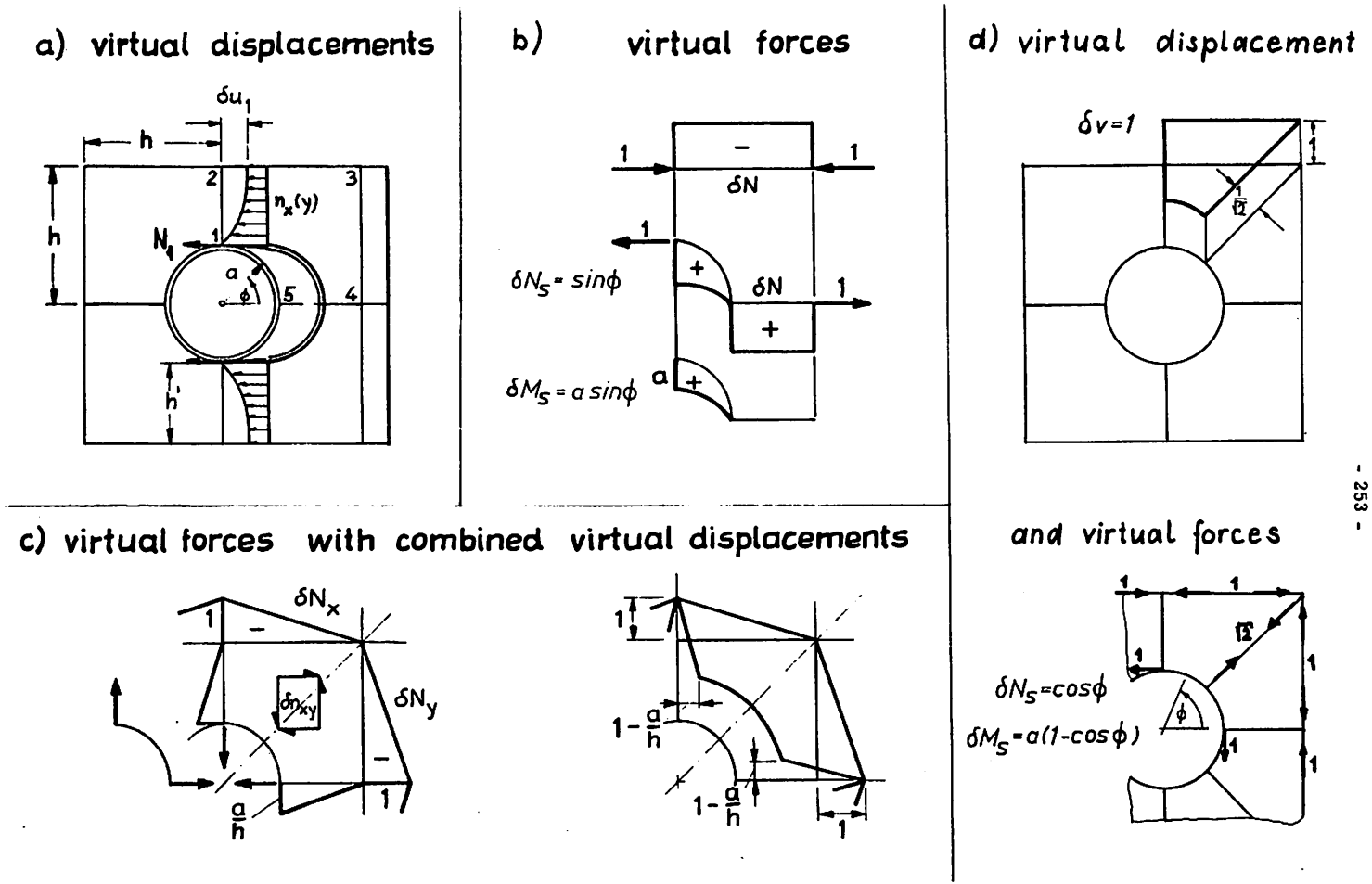

Figure 4: Virtual states in the stretching problem

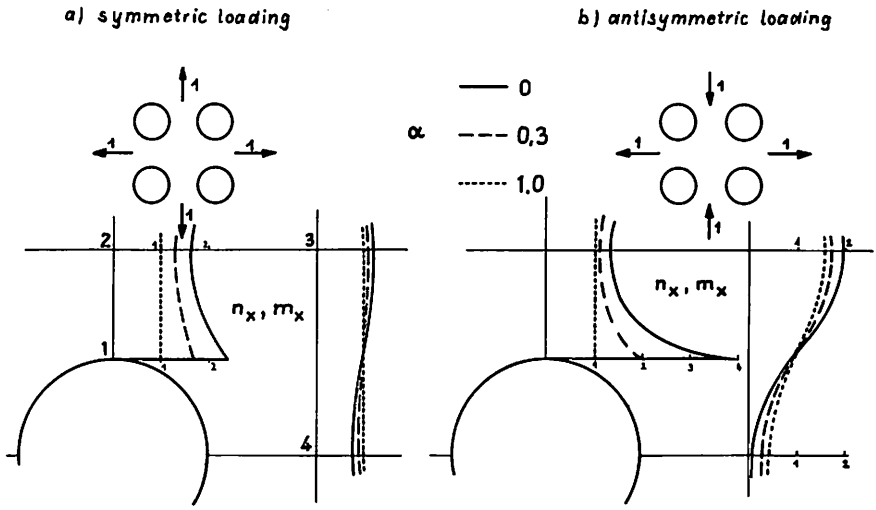

Figure 5: Stressdistribution in perforated plates with boundary stiffeners

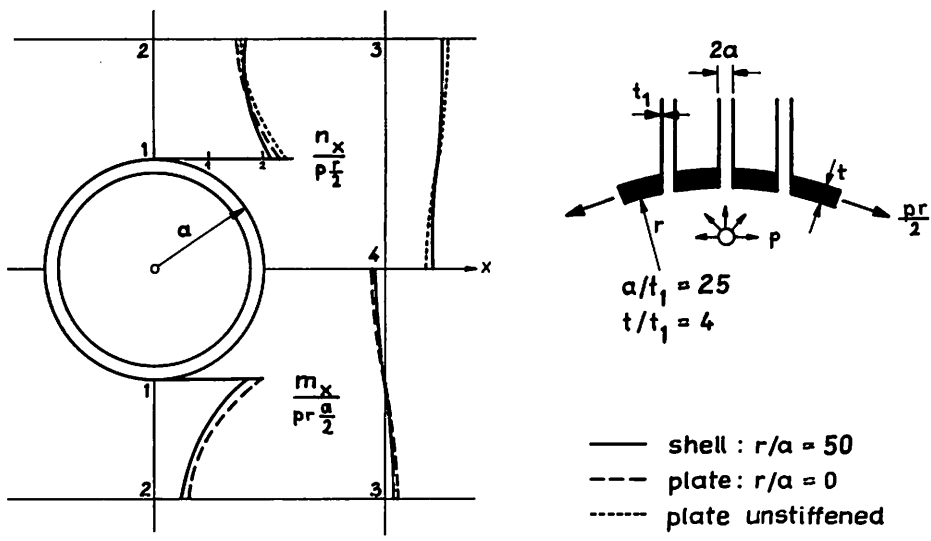

Figure 6: Perforated spherical shell

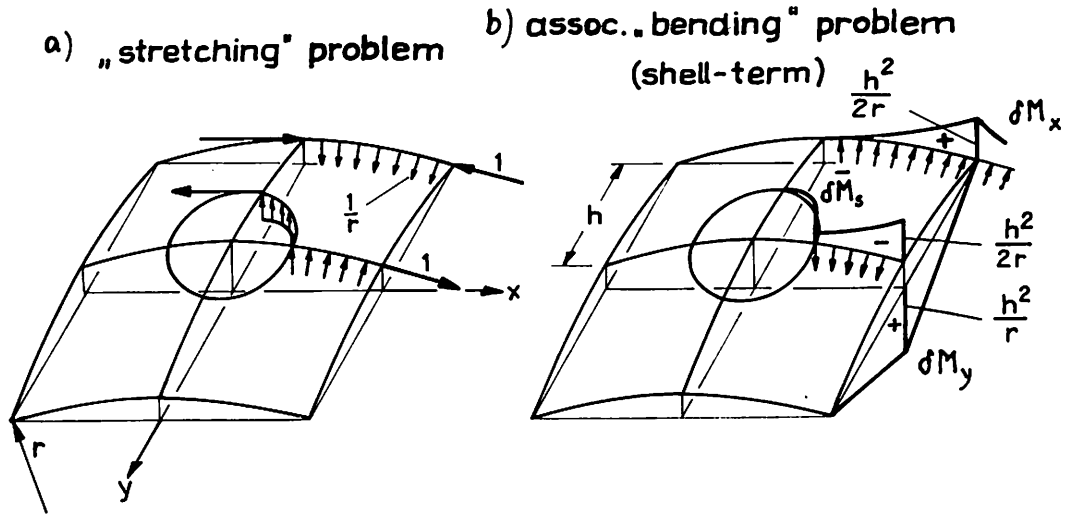

Figure 7 : Additional virtual forces in shell problems

DISCUSSION

Q J. G. LEKKERKERKER, The Netherlands

1. How did you know that one should choose a parabola in the case of uniform tension and a hyperbola in the case of shear ? I have the feeling that one should know someting about the solution to be arrived at.
2. Did you compare results with those of Dr. Meyers (doct. thesis Delft, 1967) ?

A E. GIENCKE, Germany

First, a note to the finite element analysis. If you would like to get good results, you must know something about the solution, to chose the best idealisation for your structure. From the solution for a plate with one hole we know, that the stress peak, in the case of the uniform tension increases with a second order hyperbola and the antisymmetric case with a fourth order hyperbola. The second order stress peak can be approximated by a parabola but not the fourth order peak. The comparison with the results of Dr. Meyers are given in chapter 3, they are quite well.

C D. G. H. LATZKO, The Netherlands

I should like to remind you that the applicability of the tapered hub considerations presented in the paper is by no means restricted to nuclear vessels, but on the contrary should be of direct use to the designer of high-pressure flanged closures in general, including vessels costing only a fraction of the sums you mentioned.

Q W. SCHMITT, Germany

Are you able to extend this method for calculating stress-intensity factors ?

A E. GIENCKE, Germany

By a finite method you are not able to analyze stress distribution with a singularity, apart from the singularity is specially included. That must be down.

Q C. RUIZ, U. K.

I would like to ask Prof. Giencke to amplify his statement concerning the application of his method to the determination of stress intensity factors around real cracks. I take a crack to be defined by infinite acuity or zero root radius.

A E. GIENCKE, Germany

At a crack with a zero root radius a stress singularity arises. If this well known stress singulary will be included in the analysis, by the finite method only the derivations from the introduced stress singularity due to the special boundary conditions of the problem must determined.